

AgilePilot: DRL-Based Drone Agent for Real-Time Motion Planning in Dynamic Environments by Leveraging Object Detection

Roohan Ahmed Khan, Valerii Serpiva, Demetros Aschalew, Aleksey Fedoseev, and Dzmitry Tsetserukou

Abstract—Autonomous drone navigation in dynamic environments remains a critical challenge, especially when dealing with unpredictable scenarios including fast-moving objects with rapidly changing goal positions. While traditional planners and classical optimisation methods have been extensively used to address this dynamic problem, they often face real-time, unpredictable changes that ultimately leads to sub-optimal performance in terms of adaptiveness and real-time decision making. In this work, we propose a novel motion planner, AgilePilot, based on Deep Reinforcement Learning (DRL) that is trained in dynamic conditions, coupled with real-time Computer Vision (CV) for object detections during flight. The training-to-deployment framework bridges the Sim2Real gap, leveraging sophisticated reward structures that promotes both safety and agility depending upon environment conditions. The system can rapidly adapt to changing environments, while achieving a maximum speed of 3.0 m/s in real-world scenarios. In comparison, our approach outperforms classical algorithms such as Artificial Potential Field (APF) based motion planner by 3 times, both in performance and tracking accuracy of dynamic targets by using velocity predictions while exhibiting 90% success rate in 75 conducted experiments. This work highlights the effectiveness of DRL in tackling real-time dynamic navigation challenges, offering intelligent safety and agility.

Keywords: Drone Navigation, Dynamic Environments, Motion Planning, Deep Reinforcement Learning, Safety and Agility, Computer Vision, Robotics.

I. INTRODUCTION

In recent years, autonomous drone navigation has gained significant interest, especially in the context of dynamic environments. Conventional motion planning methods, such as nonlinear Model Predictive Control (NMPC) and graph-based search algorithms, have demonstrated efficiency in structured and controlled environments but lack their capability to adapt to rapidly changing conditions in real-time. Therefore, DRL has emerged as a viable alternative, offering fast decision-making and adaptability that improve autonomous navigation. In recent work, Song et al. [1] has explored near-optimal trajectory generation in near time using DRL methods, enabling adaptation to dynamic track configurations while achieving remarkable speeds of up to 60 km/h. Another study [2] by Kaufmann et al. utilises Model Predictive Control (MPC) to navigate quickly through the track, where a convolutional network and an Extended Kalman Filter (EKF) predicts the poses of the closest gates along with uncertainty. Moreover, another breakthrough study [3] presents a SWIFT system that competes with

The authors are with the Intelligent Space Robotics Laboratory, Center for Digital Engineering, Skolkovo Institute of Science and Technology, Moscow, Russia. {roohan.khan, valerii.serpiva, demetros.aschalew, aleksey.fedoseev, d.tsetserukou}@skoltech.ru

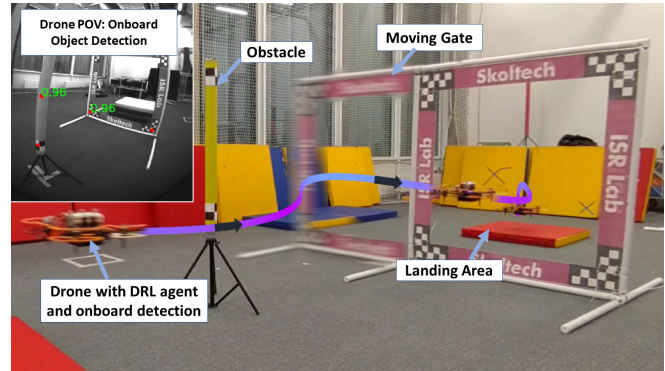


Fig. 1. AgilePilot technology performing Deep Reinforcement Learning based motion planning to avoid obstacle and navigating through moving gate and target position where objects are detected in real-time using onboard Computer Vision system

human drone pilots in drone racing by using the Proximal Policy Optimisation (PPO) algorithm to train a model that generates low-level control commands for the quadrotor. Despite these studies having developed agile systems for drones, they lack the ability to effectively avoid obstacles in real time and adapt to a highly dynamically changing environment. In addition, there are also limitations to their ability to balance safety and agility when the environment becomes highly unpredictable.

This research introduces a novel motion planner, AgilePilot, which leverages DRL to predict drone velocities for navigating dynamic environments with moving objects. The velocity prediction is situation-aware reaching up to 3.0 m/s in simpler terrain while slowing down in complex scenarios involving obstacles and moving objects. The proposed methodology involves a unique framework to train models in a simulation environment customized to achieve the level of accuracy required for Sim2Real transfer. The training is performed using Actor Critic neural network architecture and uses a unique reward structure with effective randomisation during episodes to make the application of trained models generalised and easy to implement. To track movable objects, the system applies YOLO-based object detection combined with state estimation using IPPE PnP and an EKF for robust pose estimation.

The methods used in this research revolutionise the motion planning of drones in dynamic environments by effectively adapting the velocity vector according to the complexity of terrain while taking account uncertainty in the objects movements. The broad applicability of technology is ensured by the pipeline used for training and testing of trained models

in unknown environments.

II. RELATED WORKS

Due to the overwhelming complexities of drone navigation in dynamic environments, many studies have been trying to solve the general applicability of algorithms either by using machine learning or classical methods. For example, in study [4], the policy was learnt with high uncertainty and tested in a noisy real environment. The results showed effective drone navigation in reality, but the method is applicable in 2D space only and not tested in dynamic conditions.

In study [5], DRL is utilised to avoid moving and stationary obstacles consisting of images and several scalars with Joint Neural Network (JNN). Liu et al., in research [6] use a motion planning framework that integrates visibility path searching to generate collision-free paths and RL to generate low-level motion commands. Moreover, CPU-based trained DRL for UAV to UAV tracking is introduced in [7]. The model was trained using PPO and showed considerable results. Another PPO-based learnt RL agent in study [8] was used in a racing environment as a path planner and utilized conventional Proportional–Integral–Derivative (PID) controller for controlling the motion. Moreover, Song et al. research [9] generates smooth collision-free trajectories while taking care of an unseen environment by incorporating vision with DRL. While these mentioned studies show promising capabilities for motion generation and obstacle avoidance, they have predominantly been tested in simulation environments only with less challenging scenarios.

Furthermore, in study [10] highly efficient path planner was devised for cluttered environments incorporating some extent of dynamical feasibility by adjusting time allocation based upon spatial-temporal joint optimisation. Moreover, study [11] introduced a search-based method by using a multi-stage training approach and testing the agent on real air-ground unmanned system. In [12], DRL was trained for random obstacles in dense urban environment by utilising Double Deep-Q network (DDQP) while enhancing the training stability of algorithms. In addition, study [13] improves safe navigation in obstacle avoidance by leveraging map parameterisation and low-cost planning whereas the results are validated in real-life experiments. Peter et. al in study [14] trained models using Twin-Delayed Deep Deterministic (TD3) policy gradient algorithm and real life experiments showed remarkable landing performance of drones for dynamically moving platforms in the presence of downwash and wind turbulence. The extension of these works using PPO has also been successfully implemented for multi-agents [15]. However, these approaches focus purely on path planning without considering obstacles and have only been tested on tiny-sized drones, therefore, overall restricting the high velocity potential of medium-sized drones. Lastly, another study [16] introduced OmniRace, a control interface based on drone velocity manipulation for drones of all sizes. However, its motion planning depends entirely on human input, which limits both navigation accuracy and autonomy.

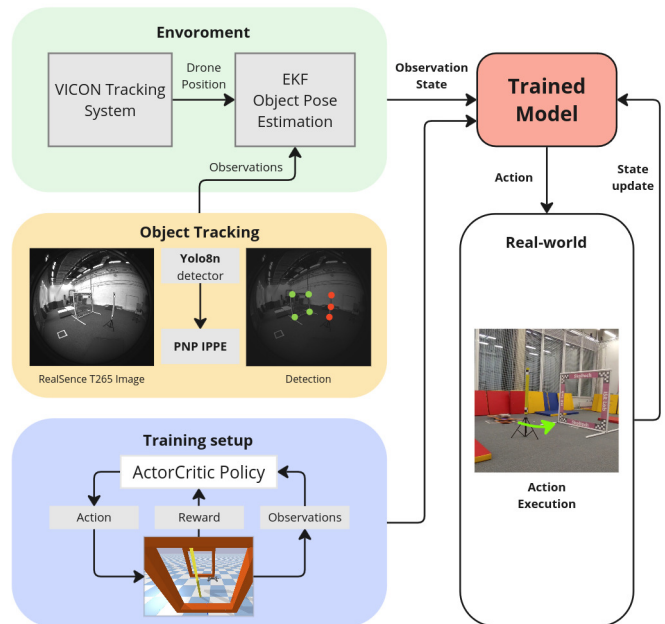


Fig. 2. AgilePilot consists of a position estimation module for the agent and dynamic objects in the environment, along with a control policy that maps state observations to control commands. The policy is trained using ActorCritic network utilising PPO algorithm in customised simulated environment. The position estimation system uses a VICON tracking system to provide the drone’s state, while object detection is performed using a YOLO neural network for gate corner detection and obstacle keypoint extraction. The keypoints are processed using IPPE PnP to estimate local positions, which are then mapped to a 3D pose in the global coordinate system.

In order to address the mentioned gaps, this research presents a novel DRL-based motion planning framework that enables velocity-based trajectory generation for any size drone due to its nature of being a model-free learning agent. Unlike previous studies that rely on static environment, our approach is designed for dynamic scenarios, ensuring robust adaptability to rapidly changing surroundings. The training environment used is Gym PyBullet [17] and carefully customised and tuned to incorporate real-world complexities for a seamless transition from simulation to reality. Furthermore, this framework accounts for dynamically evolving obstacles, allowing the drone to make intelligent decisions in real time while balancing agility and safety as required.

III. METHODOLOGY

This section explains the methods used for developing AgilePilot pipeline. Gym PyBullet is used for simulation and physics in training with PPO and models are deployed in simulated and real-life environments. The overall pipeline of our system is shown in Fig. 2.

A. Simulation Environment

The simulation setup is developed using Gym environment and PyBullet physics engine that allows realistic aerodynamics and accurate quadcopter mathematical modelling to emulate drones. We have integrated a custom midsized drone with a custom PID controller in simulation. The inertial

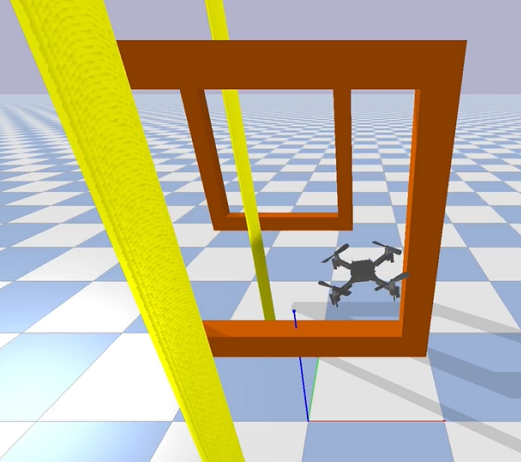


Fig. 3. Gym PyBullet simulation environment with custom objects.

and controller parameters are tuned to the level of realistic response in real environments. Moreover, custom objects such as gates and obstacles are also built, as shown in the simulation Fig. 3.

In each step, the object’s movement is governed by a random velocity drawn from a uniform probability distribution.

$$\Delta \mathbf{p} \sim \mathcal{U}(-v_{\max}, v_{\max})$$

Where $\Delta \mathbf{p} = [\Delta x, \Delta y]$ represents the change in position in the x and y directions, and $\mathcal{U}(-v_{\max}, v_{\max})$ denotes a uniform distribution over the range $-v_{\max}$ to v_{\max} .

Lastly, the PID controller allows drone to reach speed within range of ± 3 m/s in xy and ± 2 in z direction whereas rotation angles can range from $-\pi$ to π radians, by mapping desired commands to motor RPMs and subsequently to desired forces and torques by using accurate motor dynamics model.

B. Deep Reinforcement Learning

1) *Neural Network Architecture*: Our neural network follows an actor-critic shared architecture Fig. 4. The input layer consists of the following observations:

$$\hat{\mathbf{o}}_t = [\mathbf{x}_{\text{drone}}, \theta_{\text{drone}}, \mathbf{v}_{\text{drone}}, \omega_{\text{drone}}, \mathbf{d}_{\text{target}}, \Delta \mathbf{r}_{\text{obs}}]$$

where $\mathbf{x}_{\text{drone}}$ represents the drone’s position, consisting of its coordinates, θ_{drone} denotes the drone’s orientation, $\mathbf{v}_{\text{drone}}$ is the linear velocity of the drone, and ω_{drone} indicates the drone’s angular velocity. The target’s state is represented by $\mathbf{d}_{\text{target}}$, which includes the target’s 3D position, its size, and orientation. Lastly, $\Delta \mathbf{r}_{\text{obs}}$ denotes the relative position of an obstacle as well as the obstacle’s size.

The output layer of actor represents the action space, which consists of the following four values:

$$\hat{\mathbf{a}}_{t+1} = [v_x, v_y, v_z, v_{\max}]$$

where the desired velocity components of the drone are represented by v_x, v_y , and v_z , and v_{\max} denotes the maximum velocity the drone can achieve.

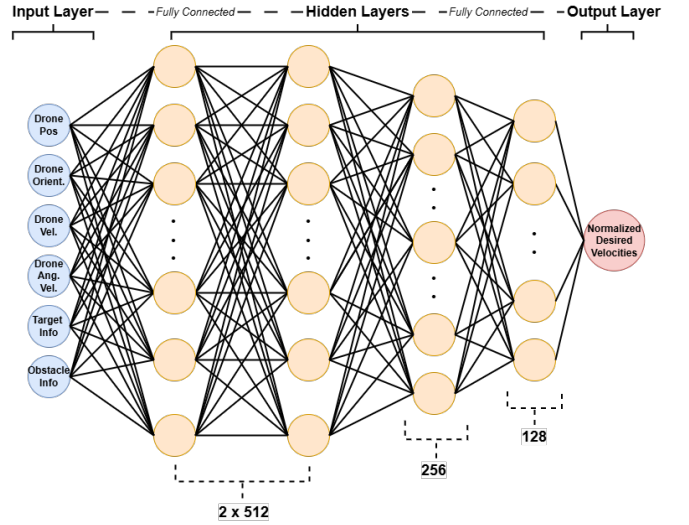


Fig. 4. Neural Network architecture representing input layer, hidden layers and output layer of our system.

The neural network is designed with ReLU activation functions and uses fully connected (FC) layers with the following structure:

$$\text{ReLU}(\text{FC}512 \times 2) \rightarrow \text{ReLU}(\text{FC}256) \rightarrow \text{ReLU}(\text{FC}128)$$

The output layer is essentially a four-dimensional velocity vector, which is controlled by a low-level PID controller. The velocity vector is tunable by some scale factor for implementation in the real-world drone control system. Moreover, the desired yaw is determined indirectly by projecting the xy velocity vector from the action space.

2) *Reward Structure*: The reward structure for the drone is designed to incentivize efficient goal traversal while avoiding obstacles Fig. 5.

The agent receives a reward based on its distance to the goal. The reward increases substantially when the drone is in close proximity to the goal which allows stable target location tracking in 3D space.

$$R_{\text{proximity}} = \frac{1}{d_{\text{goal}} + c_p},$$

where d_{goal} is the Euclidean distance between the drone’s position and the goal and c_p is the constant to avoid extremely high reward values.

Moreover, the agent is penalised for getting closer to the obstacle where the obstacles are modelled as infinite-height objects. The penalty is based on the relative distance to the obstacle and its size, using an exponential function:

$$R_{\text{obstacle}} = -c_o \cdot \exp\left(-\frac{d_{\text{obstacle}}}{r_{\text{safety}}}\right),$$

where d_{obstacle} equals $\|\Delta \mathbf{r}_{\text{obs},xyz}\|$, c_o is the penalty scaling constant, and r_{safety} is the safety region around the obstacle.

Lastly, penalties are applied either if the drone collides with an object, with a large constant, c_{penal} or if the drone’s

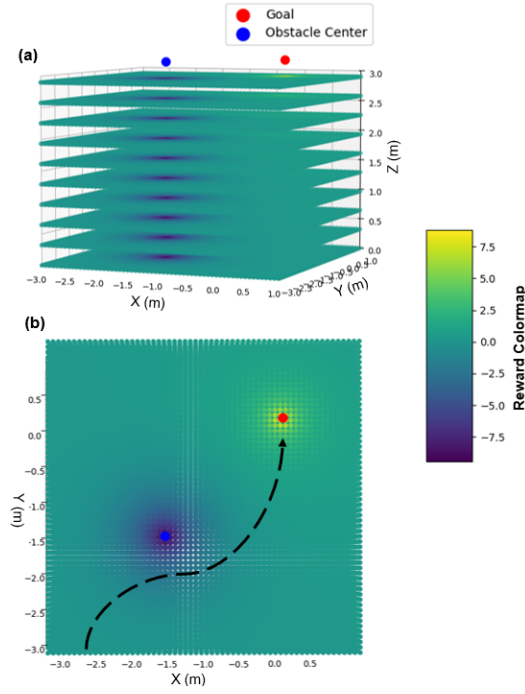


Fig. 5. Colormap visualizes reward values for drone positions in the presence of obstacle and goal in a defined area i.e., (a) shows reward structure in 3D space where obstacle is considered as infinite height and (b) shows top view in XY plane with predicted path of drone that avoids obstacle and reaches goal.

velocity is very high within the safety region to promote safe navigation behavior.

$$R_{\text{collision}} = \begin{cases} -c_{\text{penal}} & \text{if collision} \\ 0 & \text{else} \end{cases}$$

$$R_{\text{velocity}} = \begin{cases} -c_v \cdot \|\mathbf{v}\|^2 & \text{if } d_{\text{obstacle}} < r_{\text{safety}} \\ 0 & \text{else} \end{cases}$$

where $\|\mathbf{v}\|$ is the Euclidean norm of the velocity vector and c_v is the velocity penalty constant.

Finally, the total reward R_{total} is computed as:

$$R_{\text{total}} = R_{\text{proximity}} + R_{\text{obstacle}} + R_{\text{collision}} + R_{\text{velocity}}$$

3) *Training*: The drone is randomized within the following bounds:

- $x, y \in [-4.0, 4.0]$ (in the xy -plane)
- $z \in [0.3, 4.0]$ (in the z -axis)
- θ_{drone} within $[-\frac{\pi}{2}, \frac{\pi}{2}]$.

The obstacle position is randomized based on two components: longitudinal and lateral offsets.

The longitudinal offset is calculated along the line connecting the drone and the target, while the lateral offset is perpendicular to this line. Let \vec{L} be the vector from the drone to the target:

$$\vec{L} = \mathbf{d}_{\text{target}_{xyz}} - \mathbf{x}_{\text{drone}}$$

The longitudinal offset d_{long} is given by:

$$\vec{O}_{\text{long}} = d_{\text{long}} \cdot \vec{L}$$

The lateral offset is computed as the cross product of \vec{L} with the unit vector \vec{Z} :

$$\vec{L}_{\text{lat}} = \frac{\vec{L} \times \vec{Z}}{\|\vec{L} \times \vec{Z}\|}$$

The obstacle's position is then determined by combining the longitudinal and lateral offsets with drone's initial position in the episode. The z -coordinate of the obstacle is randomised within a range, typically around $z \in [0, 2]$.

TABLE I
TRAINING PARAMETERS FOR DRL

| Parameter | Value |
|------------------------|------------------------------------|
| Algorithm | PPO (Proximal Policy Optimization) |
| Total Steps | 25,000,000 |
| Number of Environments | 8 |
| Batch Size | 256 |
| Number of Steps | 2048 |
| Entropy Coefficient | 0.01 |
| Discount Factor | 0.99 |
| Clip Range | 0.2 |
| Activation Function | ReLU |

Moreover, Table I summarizes the key parameters used in the reinforcement learning algorithm within the training. The optimization algorithm used for training is Adam, which is a widely used optimizer in reinforcement learning. The learning rate is set to 1×10^{-4} .

The feature extractor (policy network) processes observations and provides the necessary features for action prediction. For PPO, the policy architecture is based on an ActorCriticPolicy which integrates both the actor (policy) and critic (value function) into a single neural network. The output layer provides a distribution of actions based on the processed input.

The model's performance is evaluated after training by running it in the environment and computing the mean and standard deviation of the rewards over multiple episodes. Fig. 6 and Fig. 7 shows mean reward and mean episode length, respectively of several trained models with different set of hyperparameters. Model 2 with hyperparameters listed in Table. I was selected for experiment due to its better convergence with highest reward and minimum episode length indicating that the policy has learned well.

C. Computer Vision System

1) *Object Detection*: The object detection system receives an image from the wide-angle Intel RealSense T265 camera with 30 fps as input and outputs an estimate of the spatial position of the gates and obstacles relative to the camera. The camera captures a frame, which is then processed by the YOLOv8n Pose neural detector. The detector identifies four key points that define the gate plane with size 1.5 x 1.5 m, as well as three key points for cylindrical obstacle with length of 1.0 m and diameter of 0.1 m. To train the detection model, a custom dataset was collected, consisting of 2,475 annotated instances of racing gates and 3,015 instances of obstacles. 4,471 images were generated from the original data set using specialized augmentation techniques. The final

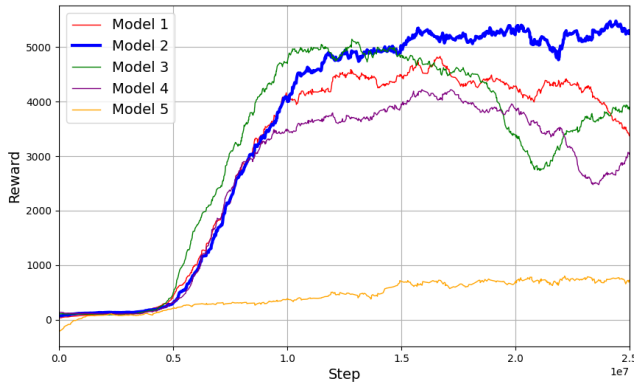


Fig. 6. Mean reward of five trained models with different parameters shows that reward increases with time before converging.

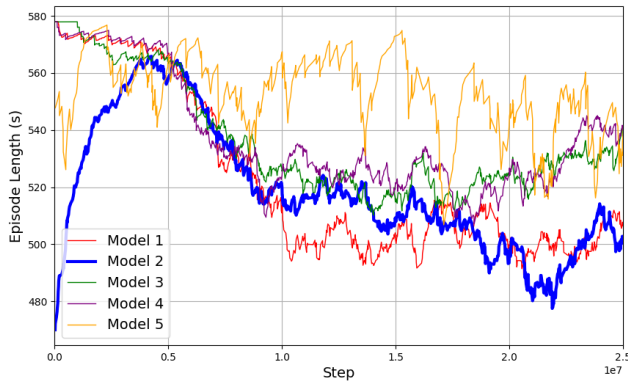


Fig. 7. Mean episode length of five trained models with different parameters shows decreasing trend with time that indicates model is converging to best learned policy

dataset was split into training, and validation sets in a 80:20 ratio. The YOLO model was trained for 500 epochs with a batch size of 32 with image resolution 424x400 px. Data augmentation was applied, including horizontal flipping with a probability of 0.5, random rotation up to 10 degrees, and color adjustments in the HSV space with the following parameters: hue 0.015, saturation 0.2, and value 0.2. The inference time of the model is 40 ms, demonstrating the system’s capability for real-time processing.

2) *Position estimation:* The Infinitesimal Plane-based Pose (IPPE) method facilitates the estimation of the spatial position and orientation of racing gates and obstacles relative to the drone’s camera. This is accomplished using the 2D coordinates of the object’s corner points, the 3D coordinates of these corners within the object’s local coordinate system and the intrinsic camera parameters. The method allows for the precise determination of the pose and orientation of the object in space. The EKF is employed to filter noisy position measurements of multiple objects, enabling accurate tracking by associating observations based on their spatial proximity. The state vector for gates is represented as $\mathbf{x} = [x \ y \ z \ \psi]^T$ and for cylindrical obstacle $\mathbf{x} = [x \ y]^T$ represent the position and orientation of an object, where:

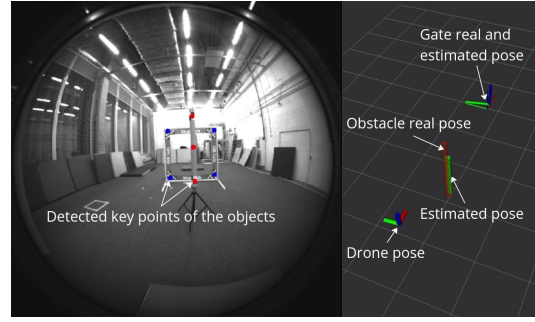


Fig. 8. The result of the detected key points on the frame and the visualization of the estimated poses of the objects in RVIZ.

x, y, z are the position coordinates, and ψ is the yaw angle (orientation). The results of the working detection and pose estimation system are presented in Fig. 8.

IV. COMPARATIVE ANALYSIS

In this analysis, we compare the performance of our DRL-based motion planner with the well-known Artificial Potential Field (APF) motion planner due to its effectiveness in dynamic environments for UAVs [18] [19]. To perform this comparison, we conducted five simulation cases to assess different dynamic conditions. The general configuration for each case includes two obstacles and one gate that the drone must pass through to reach the target location.

A. Simulation Cases

The five simulation cases are as follows:

- **Case 1:** Moving gate at 0.3 m/s with obstacle placed to exploit APF local minima.
- **Case 2:** Moving gate only at 0.3 m/s
- **Case 3:** Moving gate at 0.3 m/s with varying target height.
- **Case 4:** Both moving gate and obstacle at 0.3 m/s with varying target height.
- **Case 5:** Gate moving only at 0.6 m/s.

Each case is performed 15 times with distinctive initial drone and object positions to record the number of failures where failure exists whenever the drone is collided with the object in environment.

B. Performance Metrics

The performance metrics are given:

- **Success Rate:** The success rate is calculated using the formula:

$$\text{Success Rate} = 1 - \frac{\text{Number of Failures}}{15}$$

- **Tracking Precision:** The precision to track the moving gate and target position.
- **Time to Complete Experiment:** The total time taken for the drone to complete the full task in each case.

Table II showcases average 90% success rate out of total 75 experiments by DRL agent as compared to APF motion planner where APF completely failed to navigate through local minima situation in case 1 and struggled to complete

TABLE II
SUCCESS RATE COMPARISON OF DRL AGENT VS APF

| Case | DRL Agent | APF |
|------|-----------|-----|
| 1 | 100% | 0% |
| 2 | 100% | 80% |
| 3 | 90% | 60% |
| 4 | 80% | 40% |
| 5 | 80% | 20% |

TABLE III
PERFORMANCE METRICS FOR DRL AGENT VS APF SHOWING MEAN ERROR (ME), STANDARD DEVIATION (SD) AND TIME TAKEN (TT) TO REACH THE TARGET POINT FOR ONLY SUCCESSFUL FLIGHTS

| Case (DRL) | Tracking ME (cm) | Tracking SD (cm) | TT (s) |
|------------|------------------|------------------|--------|
| 1 | 4.80 | 0.2 | 5.00 |
| 2 | 4.30 | 0.3 | 4.50 |
| 3 | 5.50 | 0.3 | 4.20 |
| 4 | 5.50 | 0.3 | 6.40 |
| 5 | 5.60 | 0.2 | 5.20 |

| Case (APF) | Tracking ME (cm) | Tracking SD (cm) | TT (s) |
|------------|------------------|------------------|--------|
| 1 | NA | NA | NA |
| 2 | 15.6 | 1.0 | 14.7 |
| 3 | 14.2 | 0.5 | 14.8 |
| 4 | 13.4 | 1.1 | 15.5 |
| 5 | 16.0 | 1.2 | 14.0 |

its task for highly dynamically moving environment in case 4 and case 5.

Furthermore, Table III indicates key performance parameters between the two approaches. DRL agent is able to perform high precision gate and target tracking via velocity predictions i.e., approximately 3.0 times better than APF planner. Moreover, the time required to complete all the cases on average is 5.0 seconds which is approximately 3.0 times faster than APF planning in dynamic environments.

From one of the visual representation of the cases, high precision with high speed navigation is also evident from Fig. 9 where it can be seen that the drone follows through the moving gate rather smoothly and intelligently where it speeds goes beyond 2.5 m/s. On the contrary, APF planner struggles to adapt to the moving gate scenario and maintain its speed below 1.0 m/s in doing so.

V. EXPERIMENTAL EVALUATION

A. Experimental Setup

Fig. 10 illustrates the general layout of our experimental setup. The drone, with a mass of 1.80 kg, is equipped with a high-performance Intel NUC onboard computer, alongside a RealSense T265 camera for real-time object detection. The onboard computer communicates with a SpeedyBee flight controller, which is responsible for sending and receiving commands through the ArduPilot firmware. For environmental layout, obstacle, gate and landing pad are used where the objects are dynamically moved manually by a rope at speeds between 0.4-0.7 m/s to validate the transfer of simulation results to real-world conditions.

The flight tests are conducted under both static and dynamic conditions. Three test cases were designed to assess the performance of the DRL agent, specifically focusing on its velocity predictions under varying conditions and its

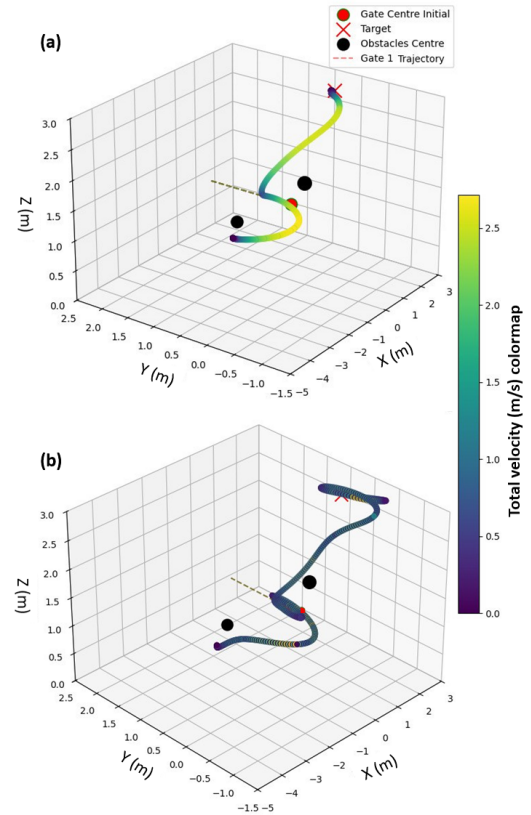


Fig. 9. Trajectory of drones with velocity colormap of drone for case 3 comparison where (a) shows trajectory using DRL agent and (b) shows trajectory via APF planning

adaptability to the changing environment. The three cases are as follows:

- **Case 1:** Slow left moving gate with obstacle and target.
- **Case 2:** Fast right moving gate with obstacle and target.
- **Case 3:** Static environment.

B. Results

1) *Objects Position Estimation:* The results of error measurements during flight experiments for the gate and obstacle pose estimation are shown in Fig. 11. For position estimation, the mean position error is 0.19 m for obstacles and 0.22 m for gates. The standard deviation for position estimation is 0.06 m for obstacles and 0.13 m for gates. In terms of orientation, the mean orientation error for gates is 0.3 radians with a standard deviation of 0.07 radians, suggesting a reasonable accuracy in orientation estimation. The root mean square error (RMSE) for position is 0.076 m for obstacles and 0.37 m for gates. Additionally, a delay in the X-coordinate position change was observed (Fig. 11 b.), ranging up to 100 ms from the time when the real pose began to change to when the predicted X-coordinate pose started to respond.

2) *Action predictions by DRL agent:* The position and velocity plots in Fig. 12 and Fig. 13 summarises that in Case 1, the gate was moved at a steady pace, allowing the drone to navigate without any abrupt changes in its motion. The agent, recognising that the environment contained moving objects, gradually increased its speed to a maximum of 1.5 m/s

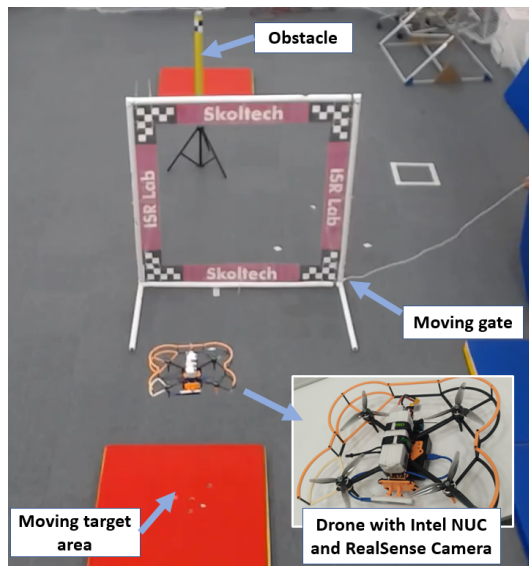


Fig. 10. Experimental layout of our system where ArduPilot drone equipped Intel NUC onboard computer and RealSense camera, performs dynamic navigation through the centre of the gate while avoiding obstacle and reaching the target point (red area).

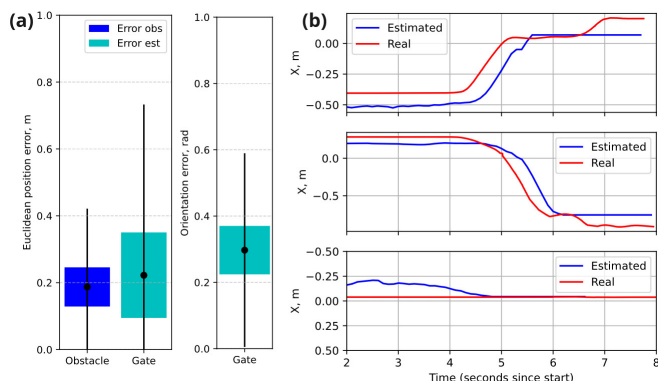


Fig. 11. (a) Euclidean position and orientation errors for gate detection. (b) Estimation of the X-coordinate position for moving gates for case 1, 2, and 3. The red line represents the ground truth X coordinated, while the blue line shows the predicted values.

while avoiding the obstacle smoothly. This smooth velocity profile suggests that the agent anticipated the gate’s motion effectively, managing to navigate without encountering any significant difficulties.

In Case 2, the gate moved much faster as the drone approached it, presenting a more dynamic scenario. To adjust, the drone increased its velocity up to 3.0 m/s in response to the rapid movement of the gate. This quick adjustment also demonstrated the gate detection system’s ability to accurately track the fast-moving gate. This behaviour specifically underscores the robustness of the agent’s velocity management in dynamic conditions.

In Case 3, with the environment remaining static, the drone’s velocity predictions were smooth and consistent throughout the flight. There were no sudden changes in the environment, which allowed the drone to maintain a steady pace. After safely passing the gate and obstacle, the drone

increased its speed, as there was no further risk of collision, leading to a more efficient and stable navigation path.

VI. CONCLUSION AND FUTURE WORK

In conclusion, we presented AgilePilot, a novel DRL-based motion planner that enables intelligent navigation in dynamic environments by leveraging real-time object detection. The DRL framework was trained in dynamic simulation environments, facilitating a robust and adaptive learning process that bridges the simulation-to-reality gap effectively. The performance of our motion planner was compared with an APF-based motion planner in simulated dynamic environments. In summary, AgilePilot outperforms the classical approach by completing the task 3 times faster and also 3 times with more accuracy than APF planner in terms of dynamic target tracking. Overall, our trained agent exhibited an average success rate of 90% out of a total 75 conducted experiments.

In the real world, three conditions were tested with varying environment and dynamic conditions by deploying the trained DRL agent onto hardware that utilized real-time object detection. The drone demonstrated safe navigation while avoiding obstacles and steadily passing through dynamic gate. However, when the environment was subject to high-speed changes, such as rapidly moving gates, the drone displayed remarkable agility and adaptability, adjusting its speed up to 3 m/s to meet the dynamic demands of the environment. The real-time detection of gates and obstacles was accurate by encompassing RMSE of 0.076 m for obstacles and 0.37 m for the moving gates. The observed delay results from the time taken for image acquisition, neural network processing, and the transformation of position and pose filtering. However, this delay does not significantly impact performance, and the drone performs well in experiments. These results validate the effectiveness of AgilePilot in real-world conditions, demonstrating its capability to navigate dynamic and unpredictable environments using real-time velocity predictions from trained agent.

In the future, more complex scenarios could be explored, including the introduction of unpredictable obstacles and environments with multiple agents. Additionally, further research could focus on fully autonomous systems that utilize CV not only for object detection but also for precise drone localization, eliminating the need for external position systems. This would improve situational awareness and expand the range of deployable scenarios for autonomous drone systems.

REFERENCES

- [1] Y. Song, M. Steinweg, E. Kaufmann, and D. Scaramuzza, “Autonomous drone racing with deep reinforcement learning,” in *2021 IEEE/RSJ International Conference on Intelligent Robots and Systems (IROS)*, 2021, pp. 1205–1212.
- [2] E. Kaufmann, M. Gehrig, P. Foehn, R. Ranftl, A. Dosovitskiy, V. Koltun, and D. Scaramuzza, “Beauty and the beast: Optimal methods meet learning for drone racing,” 05 2019, pp. 690–696.
- [3] E. Kaufmann, L. Bauersfeld, A. Loquercio, M. Müller, V. Koltun, and D. Scaramuzza, “Champion-level drone racing using deep reinforcement learning,” *Nature*, vol. 620, no. 7976, pp. 982–987, Aug 2023. [Online]. Available: <https://doi.org/10.1038/s41586-023-06419-4>

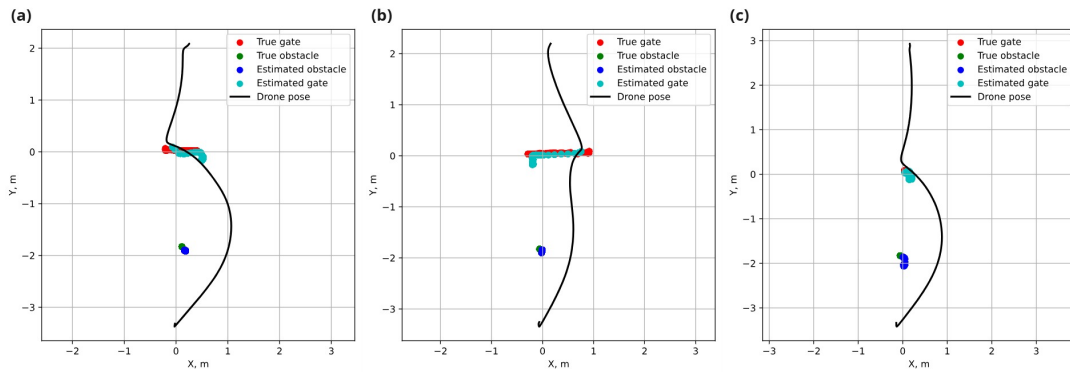


Fig. 12. Top view (XY-plane) plots of experiments where (a) shows trajectory of drone and CV detected poses of objects for case 1, (b) shows same but now includes fastly moving gate detected poses in case 2 and (c) shows trajectory of drone and object detections for static environment in case 3

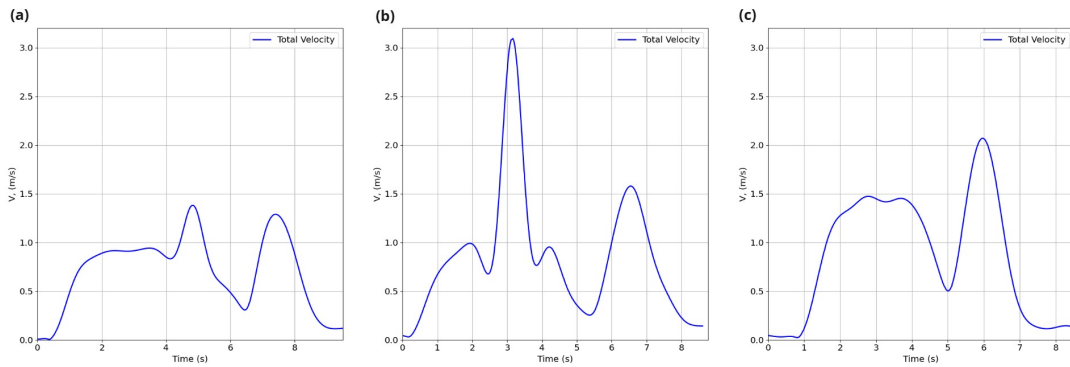


Fig. 13. Total velocities of each case where (a) shows case 1, (b) shows case 2 and (c) indicates case 3. All the velocities are shown after takeoff and before landing procedure of drone. The first maxima in each case indicates drone movement when reaching the gate and second peak highlights drone movement towards the final target point.

- [4] B. Joshi, D. Kapur, and H. Kandath, "Sim-to-real deep reinforcement learning based obstacle avoidance for uavs under measurement uncertainty," in *2024 10th International Conference on Automation, Robotics and Applications (ICARA)*, 2024, pp. 278–284.
- [5] E. Çetin, C. Barrado, G. Muñoz, M. Macias, and E. Pastor, "Drone navigation and avoidance of obstacles through deep reinforcement learning," in *2019 IEEE/AIAA 38th Digital Avionics Systems Conference (DASC)*, 2019, pp. 1–7.
- [6] Z. Liu, W. Gao, Y. Sun, and P. Dong, "A search-to-control reinforcement learning based framework for quadrotor local planning in dense environments," 2025. [Online]. Available: arXiv:2408.00275
- [7] Z. Tan and M. Karaköse, "A new approach for drone tracking with drone using proximal policy optimization based distributed deep reinforcement learning," *SoftwareX*, vol. 23, p. 101497, 2023. [Online]. Available: <https://www.sciencedirect.com/science/article/pii/S2352711023001930>
- [8] U. Ates, "Long-term planning with deep reinforcement learning on autonomous drones," in *2020 Innovations in Intelligent Systems and Applications Conference (ASYU)*, 2020, pp. 1–6.
- [9] S. Song, K. Saunders, Y. Yue, and J. Liu, "Smooth trajectory collision avoidance through deep reinforcement learning," in *2022 21st IEEE International Conference on Machine Learning and Applications (ICMLA)*, 2022, pp. 914–919.
- [10] X. Zhou, X. Wen, Z. Wang, Y. Gao, H. Li, Q. Wang, T. Yang, H. Lu, Y. Cao, C. Xu, and F. Gao, "Swarm of micro flying robots in the wild," *Science Robotics*, vol. 7, no. 66, p. eabm5954, 2022. [Online]. Available: <https://www.science.org/doi/abs/10.1126/scirobotics.abm5954>
- [11] X. Chen, Y. Qi, Y. Yin, Y. Chen, L. Liu, and H. Chen, "A multi-stage deep reinforcement learning with search-based optimization for air-ground unmanned system navigation," *Applied Sciences*, vol. 13, no. 4, 2023. [Online]. Available: <https://www.mdpi.com/2076-3417/13/4/2244>
- [12] Y. Zhu, Y. Tan, Y. Chen, L. Chen, and K. Y. Lee, "Uav path planning based on random obstacle training and linear soft update of drl in dense urban environment," *Energies*, vol. 17, no. 11, 2024. [Online]. Available: <https://www.mdpi.com/1996-1073/17/11/2762>
- [13] Y. Yang, Z. Hou, H. Chen, and P. Lu, "DRL-based Path Planner and its Application in Real Quadrotor with LIDAR," *Journal of Intelligent & Robotic Systems*, vol. 107, no. 3, p. 38, Mar. 2023. [Online]. Available: <https://doi.org/10.1007/s10846-023-01819-0>
- [14] R. Peter, L. Ratnabala, D. Aschu, A. Fedoseev, and D. Tsetserukou, "Lander.ai: Drl-based autonomous drone landing on moving 3d surface in the presence of aerodynamic disturbances," in *2024 International Conference on Unmanned Aircraft Systems (ICUAS)*, 2024, pp. 295–300.
- [15] D. Aschu, R. Peter, S. Karaf, A. Fedoseev, and D. Tsetserukou, "Marlander: A local path planning for drone swarms using multiagent deep reinforcement learning," in *2024 IEEE International Conference on Systems, Man, and Cybernetics (SMC)*, 2024, pp. 2943–2948.
- [16] V. Serpiva, A. Fedoseev, S. Karaf, A. A. Abdulkarim, and D. Tsetserukou, "Omnirace: 6d hand pose estimation for intuitive guidance of racing drone," in *2024 IEEE/RSJ International Conference on Intelligent Robots and Systems (IROS)*, 2024, pp. 2508–2513.
- [17] J. Panerati, H. Zheng, S. Zhou, J. Xu, A. Prorok, and A. P. Schoellig, "Learning to fly—a gym environment with pybullet physics for reinforcement learning of multi-agent quadcopter control," in *Proc. 2021 IEEE/RSJ International Conference on Intelligent Robots and Systems (IROS)*, 2021, pp. 7512–7519.
- [18] J. Amiryani and M. Jamzad, "Adaptive motion planning with artificial potential fields using a prior path," in *2015 3rd RSI International Conference on Robotics and Mechatronics (ICROM)*, 2015, pp. 731–736.
- [19] H. Jayaweera and S. Hanoun, "A dynamic artificial potential field (d-apf) uav path planning technique for following ground moving targets," *IEEE Access*, vol. 8, pp. 192760–192776, 01 2020.